

## Absorber Models for absorption of Carbon dioxide from sour natural gas by Methyl-diethanol Amine (MDEA)

<sup>1</sup>Akpa, Jackson Gunorubon and Okoroma, Justice U<sup>2</sup>

Department of Chemical/Petrochemical Engineering  
Rivers State University of Science and Technology,  
Port-Harcourt, Rivers State, Nigeria

### ABSTRACT

Mathematical models of the absorber for the absorption of carbon dioxide (CO<sub>2</sub>) from sour natural gas in Methyl-diethanol Amine (MDEA) solution were developed. The resulting ordinary differential model equations were solved numerically using the ode45 solver of MATLAB 7.5. The accuracy of the models was ascertained using industrial plant data from the carbon dioxide absorber of the Obiafu/Obrikom Gas Treatment plant in Rivers State, Nigeria. The models predicted the CO<sub>2</sub> concentration in the sweet gas, gas and solvent (MDEA) temperature progressions along the packed absorber. The results obtained from solutions to the models compared favorably with the plant outputs with a maximum deviation between models predictions and industrial plant outputs of 0.44%. The models were used to simulate the influence of sour gas flow rates and solvent (MDEA) concentration in solution on the performance (absorption rates of CO<sub>2</sub>) of the absorber. The results show that the absorption rate of CO<sub>2</sub> increases with increasing gas flow rate and solvent concentration.

**Keywords:** Natural gas absorption, models, Methyl Diethanol Amine (MDEA), carbon dioxide

### I. INTRODUCTION

Carbon dioxide occurs in diverse forms: it occurs naturally in oil and gas reservoirs, it is produced during the combustion of fossil fuels (coal, natural gas, gasoline and diesel) for transportation and generation of electricity; it is also released during industrial processes such as the production of cement, metal, iron and steel. The increase of the carbon dioxide concentration in the atmosphere has been identified as a major cause of global warming (McCann, 2009). Carbon dioxide reacts with hydrogen sulphide and water to form compounds corrosive to steel pipelines and gas processing equipment, its presence in natural gas decrease the heating value of the gas, it causes icing in natural gas liquids (NGL), at cryogenic conditions, carbon dioxide freezes; thus plugs natural gas processing and transportation pipelines. These show the necessity to completely eliminate carbon dioxide in natural gas as this will increase the heating value of natural gas, ensure smooth pipeline transport and efficient operations and ultimately reduce its concentration in the atmosphere.

Natural gas is a hydrocarbon gas mixture consisting of methane, varying amounts of other higher alkanes, carbon dioxide, nitrogen, and hydrogen sulfide. Natural gas has been described as the cleanest of the fossil fuels; emitting much lower amounts of soot and smog forming pollutants and no appreciable levels of mercury and other toxic substances, it is also used as a chemical feedstock in

the manufacture of plastics and other commercially important organic chemicals. The removal of carbon dioxide ensures that the natural gas meet required specification that would guarantee efficient operation of these processes.

The major processes used for carbon dioxide removal can be grouped (Maddox, 1982) as follows: Absorption Processes (Chemical and Physical absorption), adsorption Process (Solid Surface), physical separation (Membrane, Cryogenic Separation) (Karl, 2003), hybrid solution (Mixed Physical and Chemical Solvent) (David, et al., 2003).

Extensive studies on the solubility of carbon dioxide in aqueous solutions particularly amine solutions (Li and Mather, 1997; Bottoms, 1980, Desmukh and Mather, 1981; Versteeg and Van Swaaij, 1988); mixtures of amines (Kaewsichan, et al., 2001) have been performed; thus ascertain the suitability of amine solutions for absorption of carbon dioxide. Hence over the years, chemical or physical solvent absorption or a combination of both (Kohl and Nielsen, 1997) has become the preferred method for carbon dioxide removal from natural gas. Numerous experimental studies abound on absorption of carbon dioxide by solvents: (Weiland et al., 1982; Yeh and Bai, 1999), mixture of solvents: DEA and MDEA (Rinker, et al., 2000); NaOH, monoethanolamine (MEA) and 2-amino-2-methyl-1-propanol (AMP) (Tontiwachuthikul, et al., 1992); MEA and AMP (Won-Joon et al., 2009). Models for carbon dioxide and sour gas absorption in aqueous

amine solutions have also been developed by Freguia and Gray, (2003) and Kucka et al., (2003) respectively.

Most of these works have focused on experiments to determine solvent effectiveness in the absorption process and the use of various blends of solvents to achieve desired absorption. Hence this work would develop appropriate models that could predict the performance of the absorber of a typical sour natural gas treatment facility used for the removal of carbon dioxide from natural gas. The models would also be used for simulation of the absorber; thus provide a wide range of possible operating conditions for the absorption process.

## II. PROCESS DESCRIPTION

In a typical carbon dioxide absorber for sour gas treatment, the sour gas stream and liquid amine solution are contacted by countercurrent flow in an absorption tower. The sour gas to be scrubbed enters the absorber at the bottom, flows up, and leaves at the top, whereas the solvent (MDEA) enters at the top of the absorber, flows down (contacting the gas), and emerges at the bottom. The liquid amine solution containing the absorbed gas is then flowed to a regeneration unit (operated at low pressure) where it is heated and the acid gases liberated. The hot lean amine solution then flows through a heat exchanger, is contacted with rich amine solution from the contact tower and returned to the gas contact tower. A typical amine absorber is shown in Figure 1.

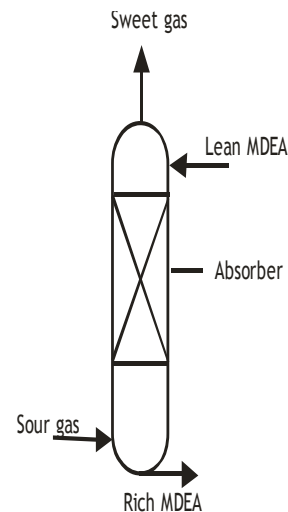


Figure 1: Schematic of the Absorber

### 2.1 Model Development

Mathematical models that could predict the performance of the absorber were developed using the principle of conservation of mass and energy. The models would predict the amount (concentration) of carbon dioxide removed from the sour gas stream and the temperature progression along the packing height of the absorber for the gas and liquid (MDEA) phases.

#### 2.1.1 Model Assumptions

The following assumptions were made in the modeling of the MDEA gas absorber. There are only two components to be transferred across the interface:  $\text{CO}_2$  and MDEA, concentration at the interface is considered as the equilibrium concentration, liquid resistance is not considered in the heat transfer process hence the temperature of the interface is the same as that of the bulk of the liquid ( $T_L$ ), the surface of heat transfer is the same as that of mass transfer, axial dispersions are insignificant and steady state condition applies. Figure 2 shows an elemental or differential section of the packed height of an absorber with its associated inflow and outflow streams.

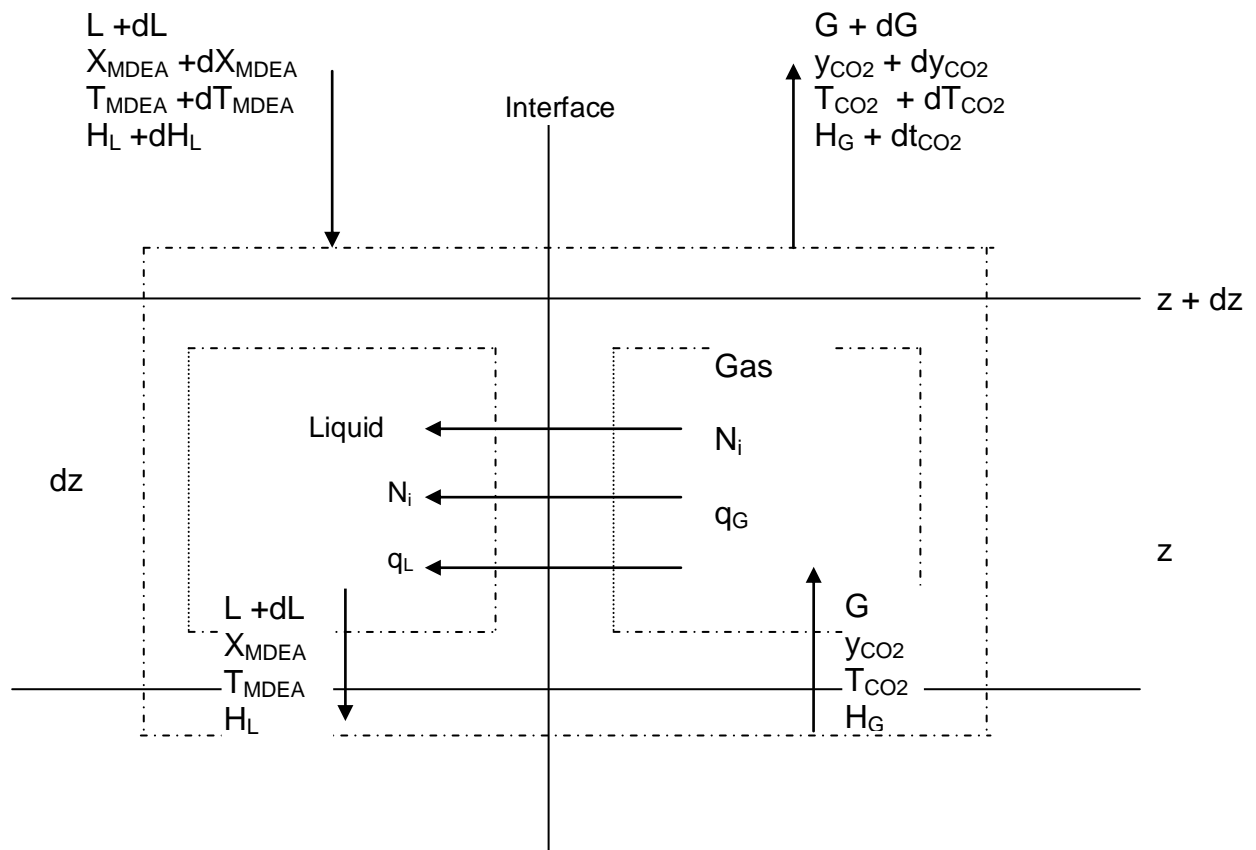


Figure 2: Mass and heat transfer in differential section of the Absorber

With these assumptions, the gas and liquid phase mass and energy balance for a differential packing of the absorber as shown in Figure 2 results in the following equations:

**Mass Balance**

1. Gas: CO<sub>2</sub>:

$$\frac{dY_{CO_2}}{dz} = -\frac{K_G(Y_{CO_2} - Y_{CO_2,e})a}{G} \quad (1)$$

2. Liquid: MDEA:

$$\frac{dX_{MDEA}}{dz} = -\frac{K_{MDEA}(X_{MDEA} - X_{MDEA,e})a}{G} \quad (2)$$

**Energy (Enthalpy) Balance**

1. Gas Phase

$$\frac{dT_G}{dz} = \frac{-h_G a(T_G - T_L)}{G(C_{P_B} + Y_{CO_2} C_{P_{CO_2}} + X_{MDEA} C_{P_{MDEA}})} \quad (3)$$

2. Liquid Phase

$$\frac{dT_L}{dz} = -\left[GC_{P_{CO_2}}(T_G - T_0) + GH_{OS}\right] \frac{K_G(Y_{CO_2} - Y_{CO_2,e})a}{GLC_{P_L}} - \left[GC_{P_{MDEA}}(T_G - T_0) - GH_V\right] \frac{K_{MDEA}(X_{MDEA} - X_{MDEA,e})a}{GLC_{P_L}} - \frac{h_G a(T_G - T_L)}{LC_{P_L}} \quad (4)$$

Where: a is specific interfacial surface area, G is molar gas flux, K<sub>G</sub> is gas film transfer coefficient, Y<sub>CO<sub>2</sub></sub> is mole fraction of carbon dioxide in gas phase, Y<sub>CO<sub>2</sub>,e</sub> is equilibrium mole fraction of CO<sub>2</sub> in gas phase, X<sub>MDEA</sub> is mole fraction of MDEA in gas phase, X<sub>MDEA,e</sub> is equilibrium mole fraction of MDEA in gas phase, L is Liquid molar flux, T<sub>G</sub> is gas phase temperature, T<sub>L</sub> is liquid phase temperature, C<sub>P<sub>i</sub></sub> is heat capacity of component i, H<sub>OS</sub> is heat of solution, H<sub>V</sub> is heat of vaporization of MDEA, h<sub>G</sub> is heat transfer coefficient of gas phase.

## 2.2 Methodology

The models were developed using the principles of conservation of mass and energy as presented in Appendix 1. The accuracy of the models was tested with industrial data from the carbon dioxide absorber of the Nigerian Agip Oil Company Obiafu/Obrikom Gas Treatment plant in Rivers State, Nigeria. The developed models were then used to study the effects of certain process parameters on the performance of the absorber.

### 2.2.1 Determination of Process parameters and operating conditions

To solve the model equations of the absorber (eqns. (1), (3) and (4)) requires the determination of certain constants, physical properties and compositions of natural gas, carbon dioxide and MDEA. These properties were determined as follows: Absorber properties, physical properties and compositions of natural gas, carbon dioxide and MDEA were obtained from the Nigerian Agip Oil Company (NAOC) Obiafu/Obrikom (OB/OB) gas treatment plant in Rivers state and are tabulated in Tables 1 and 2. Other parameters in the model equations were obtained from relevant literatures as listed in Table 3.

Table 1: Properties of absorber feedstock and products (NAOC OB/OB Gas Plant data)

| Property                                 | Inlet  | Outlet  |
|--|--------|---------|
| Gas Temperature (K)                      | 313.67 | 325.11  |
| Liquid (MDEA) Temperature (K)            | 313.40 | 316.33  |
| CO <sub>2</sub> mole fraction (mol/mol%) | 0.0167 | 0.00000 |

Table 2: Absorber operating conditions

| Parameter   | Symbol       | Value  | Unit                           |
|---|--------------|--------|--------------------------------|
| Molar gas flux  | $G$          | 0.0148 | kmol/m <sup>2</sup> s          |
| Molar liquid flux   | $L$          | 0.0095 | kmol/m <sup>2</sup> s          |
| Equilibrium mole fraction of CO <sub>2</sub> in gas phase | $y_{CO_2,e}$ | 0.191  | Unitless                       |
| Equilibrium mole fraction of MDEA in gas phase            | $X_{MDEA,e}$ | 0.325  | Unitless                       |
| Height of column  | $z$          | 20     | M                              |
| Specific interfacial surface area                         | $a$          | 416    | m <sup>2</sup> /m <sup>3</sup> |
| Reference Temperature                                     | $T_o$        | 298    | K                              |

Table 3: Properties of gas and liquid solvent

| Parameter                                 | Symbol       | Value             | Unit                  | Reference                       |
|---|--------------|-------------------|-----------------------|---------------------------------|
| Gas – film transfer coefficient           | $K_G$        | 0.000096          | kmol/m <sup>2</sup> s | Karl, 2003                      |
| Liquid – film transfer coefficient        | $K_{L,MDEA}$ | 0.000051          | kmol/m <sup>2</sup> s | Karl, 2003                      |
| Gas phase Heat transfer coefficient       | $h_G$        | 0.01              | KJ/m <sup>2</sup> sK  | Karl., 2003                     |
| Enthalpy of gas phase                     | $H_G$        | 19000             | KJ/kmolK              | Karl, 2003                      |
| Enthalpy of liquid phase                  | $H_L$        | 26000             | KJ/kmolK              | Karl, 2003                      |
| Specific heat Capacity of CO <sub>2</sub> | $C_{pCO_2}$  | 37.13             | KJ/kmolK              | Karl, 2003                      |
| Specific heat Capacity of liquid          | $C_{pL}$     | 49.982            | KJ/kmolK              | Karl, 2003                      |
| Specific heat Capacity of MDEA            | $C_{pMDEA}$  | 49.982            | KJ/kmolK              | Tontiwachwuthikul, et al (1992) |
| Specific heat Capacity of gas             | $C_{pB}$     | 37.13             | KJ/kmolK              |                                 |
| Heat of solution for CO <sub>2</sub>      | $H_{OS}$     | $3.9 \times 10^5$ | KJ/kmolK              |                                 |
| Heat of vaporization of MDEA              | $H_V$        | $2.6 \times 10^4$ | KJ/kmolK              |                                 |

### 2.2.2 Solution Technique of Model Equations

The MatLab 7.5 ODE45 solver from Mathworks for non-stiff ordinary differential equations which uses the 4<sup>th</sup> order RungeKutta algorithm was employed in solving the resulting ordinary differential model equations.

## III. RESULTS AND DISCUSSION

The results obtained from the solution of the model equations are presented as follows:

### 3.1 Carbon dioxide concentration along absorption column height

The model prediction of the concentration of carbon dioxide in the sweet natural gas stream as it flows up the absorber is shown in Figure 3.

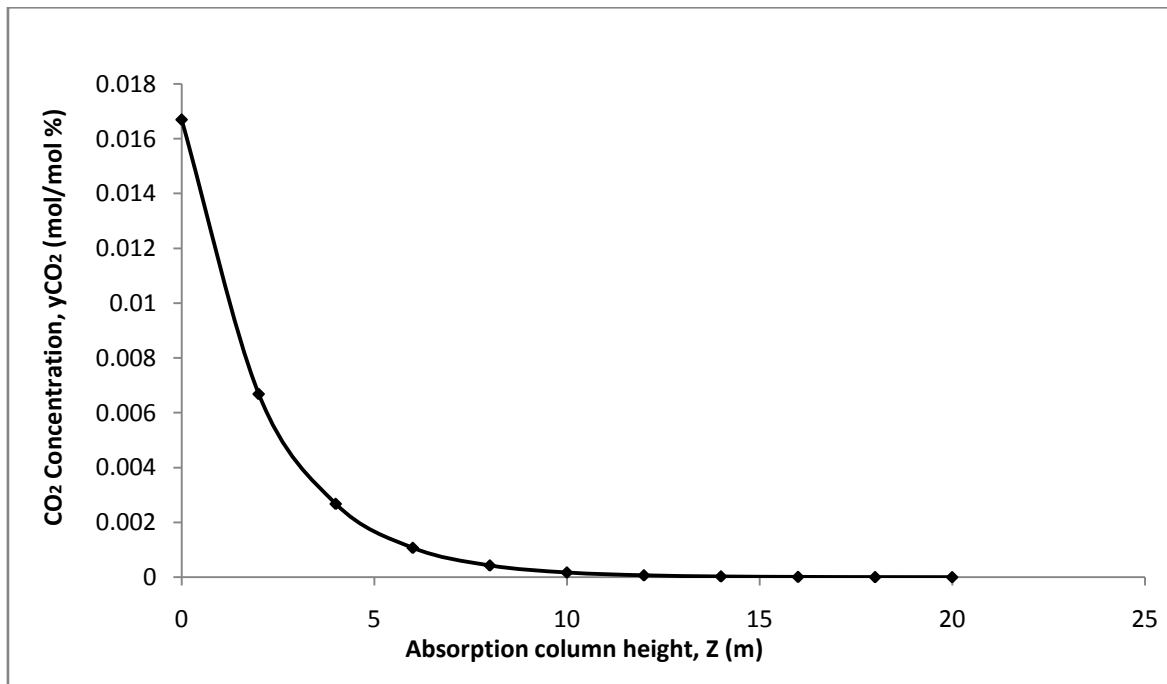


Figure3: Variation of gas CO<sub>2</sub> concentration(mole fraction) from bottom of column

Figure 3 shows that the carbon dioxide concentration in the natural gas stream reduces as the gas flows from the bottom of the column to the top. Model results show that about 93.6% of the carbon dioxide absorption occurred in the first 6 meters of the column. Thereafter, the absorption rate increased very minimally and the concentration of carbon dioxide became virtually constant from a height of approximately 10 meters and above.

### 3.2 Gas and Liquid stream temperatures across the absorption column height

The temperature progressions of the gas and liquid streams as both streams flow up and down the absorption column respectively are depicted in Figure 4.

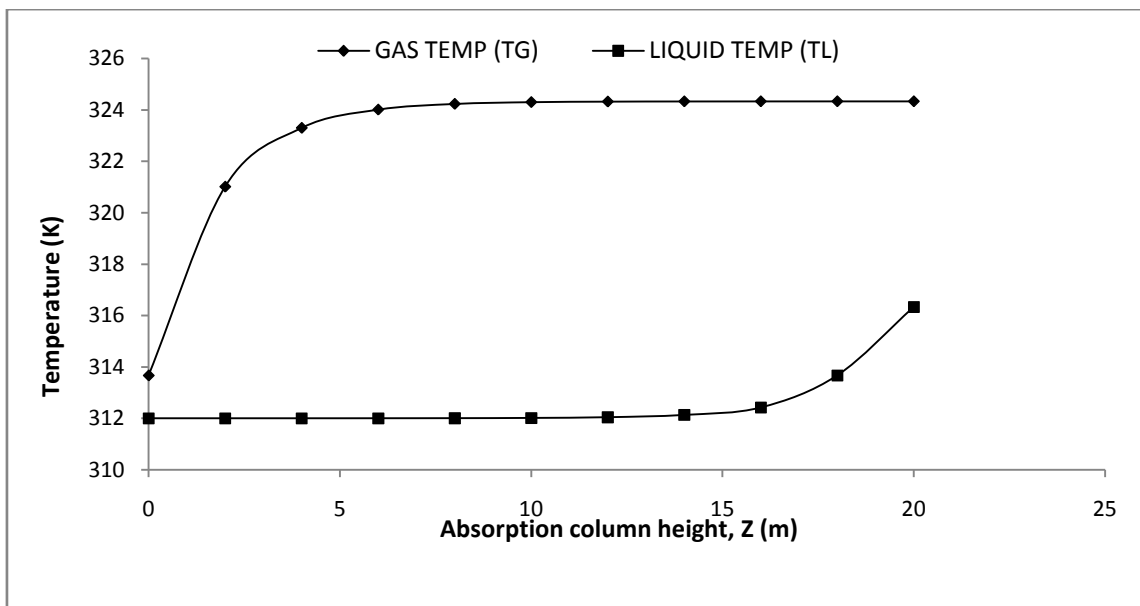


Figure 4: Gas and Liquid stream temperatures along the absorption column height.

Figure 4 shows that the temperature of the absorbing solvent, Methyl-diethanol Amine (MDEA) decreased sharply at the top 4 meters then gradually and finally becomes constant as it flows from the top to the bottom of the column; while the temperature of the natural gas stream increased sharply at the first/bottom 4 meters, then gradually and finally becomes constant as it flows from the bottom to the top of the column. The liquid

temperature decreased due to the heat of solution released between carbon dioxide and MDEA while the gas temperature increased due to heat transfer between the gas and liquid phases. The increase in gas temperature could decrease the viscosity of the solution and decrease the solubility of carbon dioxide in MDEA liquid. The former phenomenon has been reported by Daneshvar, et al., (2005) to dominate over the later resulting in increased rate of absorption as can be seen in Figure 3. Similar finding was reported by Saha et al., (1993) for the absorption of carbon dioxide in 2-amino-2-methyl-1-propanol (AMP). Also, the slope in the gas temperature curve is the same as that of the carbon dioxide concentration.

### 3.3 Model Validation

A comparison of the model predictions and the outputs of the absorber from the NAOC OB/OB Gas Plant of the carbon dioxide concentration in sweet natural gas, natural gas and MDEA liquid temperatures are presented in Table 3.

Table 3: Comparison of model predictions and absorber outputs

| Process Parameter             | Model Prediction | Plant Data | % Deviation |
|-------------------------------|------------------|------------|-------------|
| CO <sub>2</sub> concentration | 0.00000          | 0.00000    | 0.00        |
| Gas Outlet Temperature (K)    | 324.32           | 325.11     | 0.24        |
| MDEA Outlet Temperature (K)   | 312.00           | 313.40     | 0.44        |

Table 3 shows the accuracy of the models in predicting these parameters for the absorber in the Nigerian Agip Oil Company Obiafu/Obrikom gas plant as the maximum deviation between model predictions and industrial plant outputs is 0.44%. Therefore the model equations developed can be used effectively to simulate the absorber of the NAOC OB/OB gas plant.

### 3.4 Process Simulation

The effects of sour natural gas flow rate and concentration of the solvent (DMEA weight %) on the performance of the absorber using the models developed were investigated.

#### 3.4.1 Effect of Gas flow rate

Figure 5 shows the effects of varying the sour gas flow rate on the performance of the absorber.

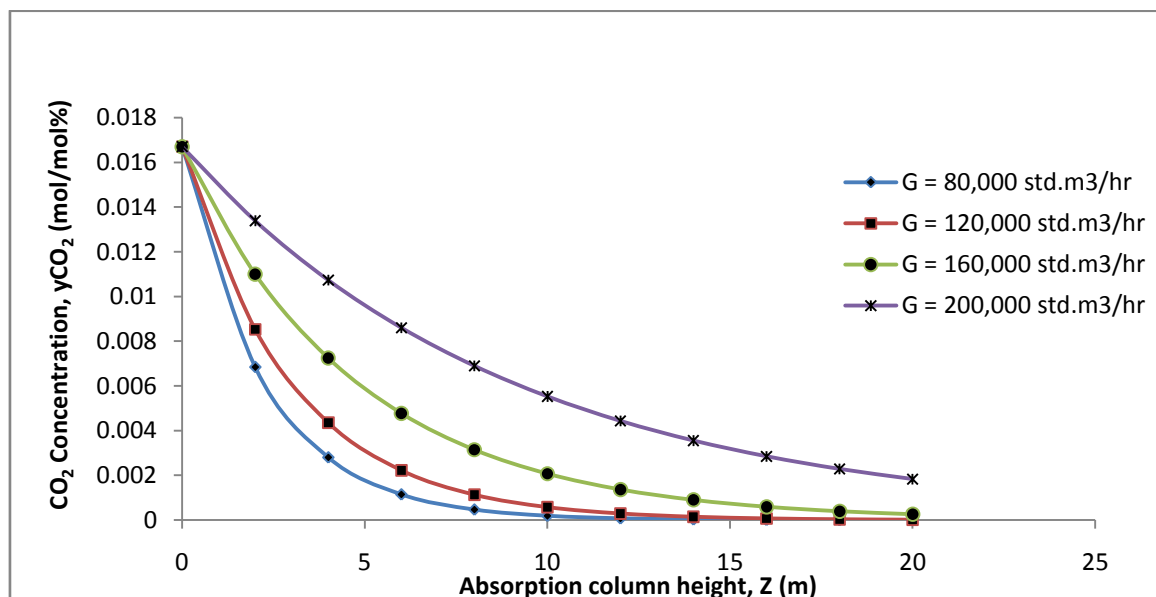


Figure 5: Carbon dioxide concentration along column height for different gas flow rates.

When the gas flow rate is increased, the gas flows faster, spends less time in the column and the contact time with the DMEA solvent is reduced; hence less carbon dioxide gas is adsorbed and the rate of absorption decreased. These trends the model predicts accurately as shown in Figure 5 where the outlet concentration of carbon dioxide in the sweet natural gas increase with increase in sour gas flow rate, indicating a decrease in absorption rate along the column with increase in gas flow rate. A three dimensional surface plot of these trends is further demonstrated in Figure 6.

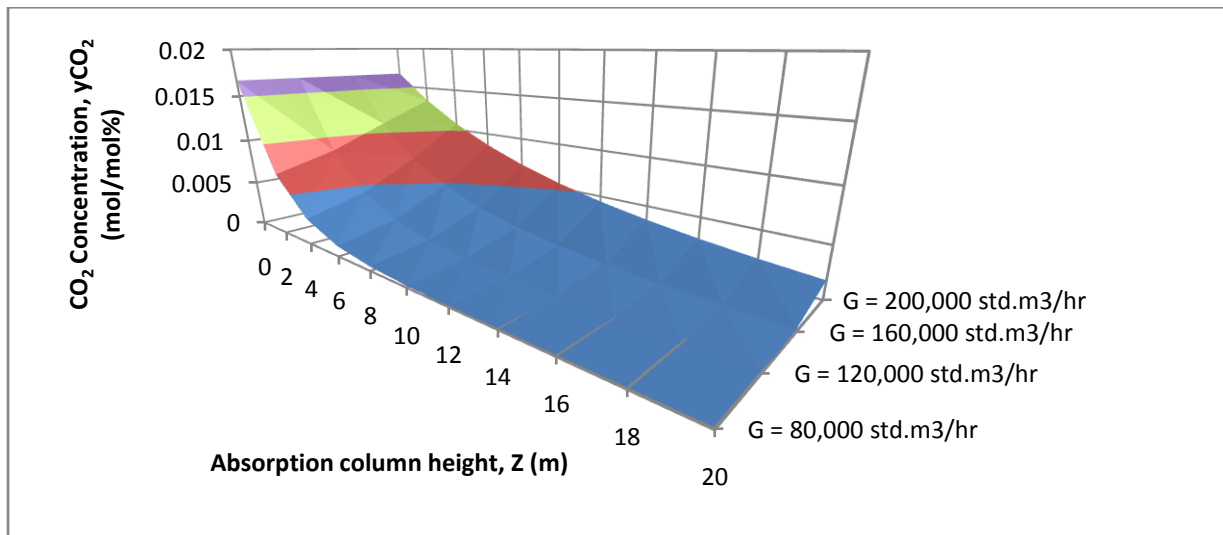


Figure6: Surface plot of CO<sub>2</sub> concentration through column height at different gas flow rates

### 3.4.2 Effect of MDEA concentration (weight %)

The effects of methyl di-ethanol amine concentration (MDEA) on the performance of the absorber (treatment of feed sour gas with different amine concentrations and the observed % mole concentration of carbon dioxide in the sweet gas) are shown in Figure 7. Figure 7 shows a general decrease in concentration of carbon dioxide in the sweet gas as the concentration of amine increases. This decrease has been attributed by Daneshver, et al., (2005) to be due to the increase in amine solvent capacity with increase in concentration of amine in the solution.

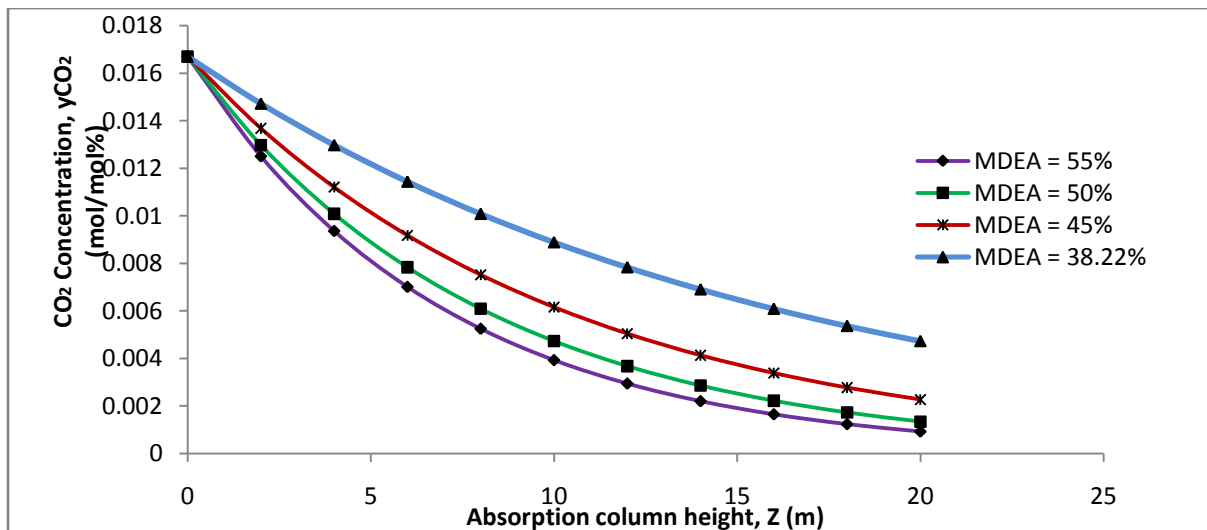


Figure 7: Effect of concentration of MDEA on carbon dioxide concentration

Figure 7 also shows an initial sharp increase in the rate of absorption (decrease in carbon dioxide concentration in sweet gas) with increase in MDEA concentration (38.22 - 45wt% MDEA). The increase in absorption rate reduced with further increase in concentration of MDEA (45 - 55wt% MDEA). These trends are similar to those reported by Won-Joon et al., (2009) where increase in absorbent concentration of 10 - 40wt% in monoethanolamine (MEA) and 2-amino-2-methyl-1-propanol (AMP) increased carbon dioxide removal efficiency. Removal efficiency then decreased at higher concentrations (> 40wt %) of the absorbents. Similar trends in absorption rates were also reported by Yeh and Bai (1999). The trends in Figure 7 showing the high increase in absorption rates with initial increase in MDEA concentration (sharp drop in outlet concentrations of carbon dioxide in the sweet gas stream) which gradually decrease with subsequent increase in MDEA concentrations are shown vividly in Figure 8 and in a three dimensional surface plot in Figure 9. The surface plot shows a steep transient in the carbon dioxide concentration at the lower part of the column which progressed gradually and become virtually constant at the top of the column.

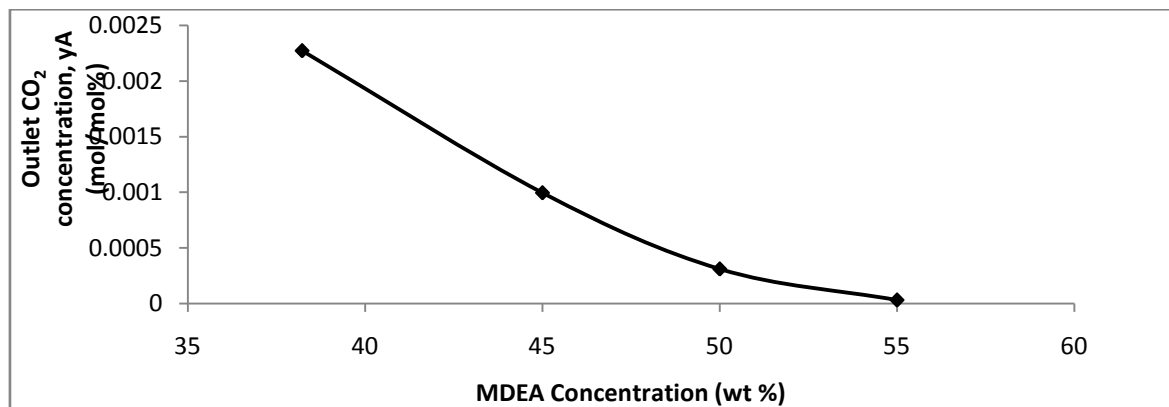


Figure 8: Plot showing the effect of MDEA concentration on the outlet CO<sub>2</sub> concentration

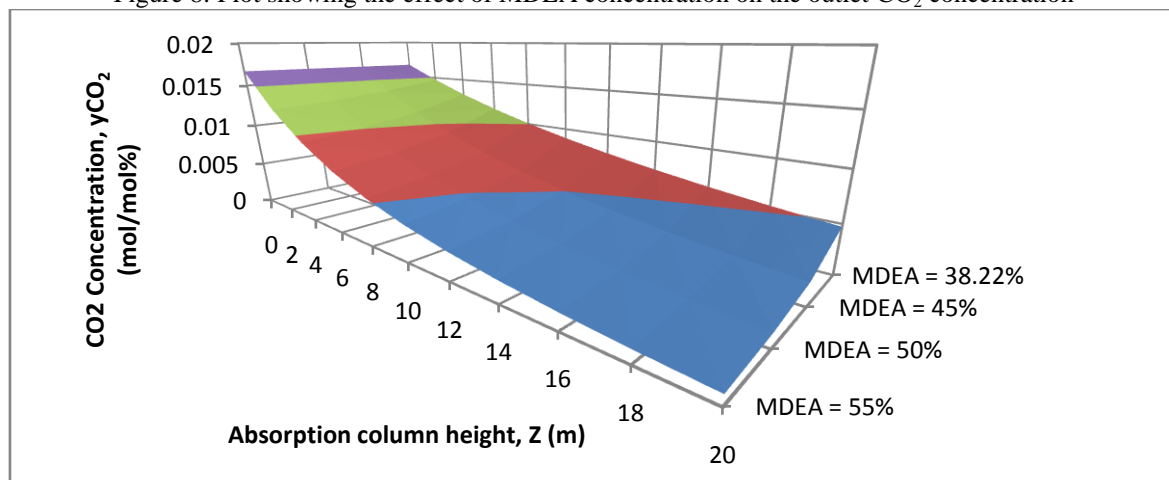


Figure 9: Surface plot of CO<sub>2</sub> concentration along column height at varying concentrations of MDEA

#### IV. CONCLUSION

Detailed models of the absorber for the absorption of carbon dioxide in sour natural gas using methyl diethanol amine (MDEA) have been developed. The models predicted accurately the concentration of carbon dioxide in the sweet gas and the temperature progression of the gas and liquid (solvent) streams along the absorber. Results from models developed using plant data from the Nigerian Agip Oil Company Obiafu/Obrikom gas treatment plant shows that the maximum deviation between model predictions and industrial plant outputs was 0.44%. The models were used to simulate the effects of sour gas flow rates and solvent (MDEA) concentration in solution on the performance of the absorber.

#### V. NOMENCLATURE

|                |  |
|----------------|--|
| $a$            | Specific interfacial surface area ( $\text{m}^2/\text{m}^3$ )                            |
| $C_L$          | Specific heat of liquid (KJ/kmolK)   |
| $C_{p_B}$      | Specific heat of gas (KJ/kmolK)  |
| $C_{p_{CO_2}}$ | Specific heat of CO <sub>2</sub> (KJ/kmolK)  |
| $C_{p_{MDEA}}$ | Specific heat of MDEA (KJ/kmolK)   |
| $G$            | Molar gas flux or gas phase molar velocity ( $\text{kmol}/\text{m}^2\text{s}$ )          |
| $h_G$          | Heat transfer coefficient of gas phase ( $\text{KJ}/\text{m}^2\text{sK}$ )               |
| $H_G$          | Enthalpy of gas phase (KJ/kmolK)   |
| $H_L$          | Enthalpy of liquid phase (KJ/kmolK)  |
| $H_{OS}$       | Heat of reaction – include heat of solution for CO <sub>2</sub> (KJ/kmolK)               |
| $H_V$          | Heat of vapourization of MDEA (KJ/kmolK)   |
| $K_G$          | Gas – film transfer coefficient in terms of mole fraction ( $1/\text{m}^2\text{s}$ )     |
| $K_{L,MDEA}$   | Liquid – film transfer coefficient in terms of mole ( $\text{kmol}/\text{m}^2\text{s}$ ) |
| $L$            | Molar liquid flux ( $\text{kmol}/\text{m}^2\text{s}$ )                                   |
| $T_G$          | Temperature of gas phase (K)   |
| $T_L$          | Temperature of liquid phase (K)  |

|              |   |
|--------------|---|
| $T_o$        | Reference temperature (K)   |
| $X_{MDEA}$   | Mole fraction of MDEA in the gas phase                                |
| $X_{MDEA,e}$ | Equilibrium (interface) mole fraction of MDEA in gas phase            |
| $y_{CO_2}$   | Mole fraction of CO <sub>2</sub> in the gas phase                     |
| $y_{CO_2,e}$ | Equilibrium (interface) mole fraction of CO <sub>2</sub> in gas phase |
| $z$          | Height of column (m)  |

## REFERENCES

- [1.] Bottoms, W.B., 1980. Correlation and prediction of the solubility of carbon dioxide in aqueous alkanolamine and mixed alkanolamine solutions, *Industrial and Engineering Chemistry Research*, 41: 1658–1665.
- [2.] Daneshvar, N., D. Salari, M.Z. Zamzami and S. Aber, 2005. Absorption of carbon dioxide into aqueous solutions of N, N-dimethylethanolamine and aqueous blends of mono and diethanolamine, *Chem. Biochem. Eng. Q.*, 19 (13): 297-302.
- [3.] David, C., B. Kellogg, and S. Pankaj, 2003. "LNG A Proven Stranded Gas Monetization Option" SPE Paper (84252): pp: 3.
- [4.] Desmukh, R.D. and A.E. Mather, 1981. A mathematical Model For Equilibrium Solubility of Hydrogen Sulfide and Carbon Dioxide in Aqueous Alkanolamine Solutions, *Chem. Eng. Sci.*, 36:355-362.
- [5.] Freguia, U.O. and T.R. Gary, 2003. Modeling of CO<sub>2</sub> Capture by Aqueous Monoethanolamine, *AIChE Journal*, (49),7: 1676-1686.
- [6.] Kaewsichan, L., O. Al-Bofersen, V.F. Yesavage and M. Sami Selim, 2001. Predictions of the solubility of acid gases in monoethanolamine (MEA) and methyldiethanolamine (MDEA) solutions using the electrolyte-Uniquac model, *Fluid Phase Equilibria*, 183: 159-171.
- [7.] Karl, A.H. 2003. Modelling and experimental study of CO<sub>2</sub> absorption in a membrane contactor, Thesis – NUST, pp: 102.
- [8.] Kohl, A. and R. Nielsen, 1997. *Gas Purification*, 5th edition, Gulf Publishing Company.
- [9.] Kucka, L., I. Muller, E. Kenig and A. Gorak, 2003. On the modelling and simulation of sour gas absorption by aqueous amine solutions. *Chem. Eng. Sci.*, 58: 3571-3578.
- [10.] Li, Y. G., and A. E. Mather, 1997. Correlation and prediction of the solubility of CO<sub>2</sub> and H<sub>2</sub>S in aqueous solutions of methyldiethanolamine, *Industrial and Engineering Chemistry Research*, 36: 2760-2765.
- [11.] Maddox, R. N., 1982. *Gas Conditioning and Processing – Advanced Techniques and Applications*, Ed.: Campbell, J. M., Campbell Petroleum Series, Norman, Okla. pp: 370.
- [12.] McCann N., D. Phan, X. Wang, W. Conway and R. Burns, 2009. Kinetics and mechanism of carbamate formation from CO<sub>2</sub> (aq), carbonate species, and monoethanolamine in aqueous solution, *The Journal of Physical Chemistry A*, 113: 5022-5029.
- [13.] NAOC OB/OB Gas Plant Data, 2006. Agip KCO Training Special Project, OJT Technical Workbook – Obiafu/Obrikom Gas Plant.
- [14.] Rinker, E.B., S.S. Ashour, H.A. Al-Ghawas and O.C. Sandall, 2000. Absorption of CO<sub>2</sub> into aqueous blends of DEA and MDEA. *Ind. Eng. Chem. Res.*, 39: 4346-4356.
- [15.] Saha, A.K., S.S. Bandyopadhyay, P. Saju and A.K. Biswas, 1993. Selective removal of hydrogen sulfide from gases containing hydrogen sulfide and carbon dioxide by absorption into aqueous solutions of 2-amino-2-methyl-1-propanol, *Ind. Eng. Chem. Res.* 32 (12): 3051–3055.
- [16.] Tontiwachwuthikul, P., A. Meisen and J. Lim, 1992. CO<sub>2</sub> absorption by NaOH, Monoethanolamine and 2-Amino-2-Methyl-1-Propanol solution in a packed column, *Chemical Engineering Science*, 47 (2): 381-390.
- [17.] Versteeg, G.F. and W.P.M Van Swaaij, 1988. Solubility and Diffusivity of Acid Gases (CO<sub>2</sub>, N<sub>2</sub>O) in Aqueous Alkanolamine Solutions *Journal of Chemical Engineering*, volume 33: 29-34.
- [18.] Weiland, R.H., M. Rawal and R.G. Rice, 1982. Stripping of Carbon Dioxide from Monoethanolamine Solutions in a Packed Column, *AIChEJ*, 28:963-973.
- [19.] Won-Joon, C., S. Jong-Beom, J. Sang-Yong, J. Jong-Hyeon and O. Kwang-Joong, 2009. Removal characteristics of CO<sub>2</sub> using aqueous MEA/AMP solutions in the absorption and regeneration process, *Journal of Environmental Sciences*, 21: 907–913
- [20.] Yeh, A.C. and H. Bai, 1999. Comparison of ammonia and monoethanolamine solvents to reduce CO<sub>2</sub> greenhouse gas emissions. *Science of the Total Environment*, 228: 121– 133.
- [21.] Yih, S.M. and C.C. Sun, 1987. Simultaneous Absorption of hydrogen Sulfide and Carbon dioxide into Di-isopropanolamine solution, *The Canadian Journal of Chemical Engineering*, 65:581 - 585.

**APPENDIX I**

The steady state mass balance on a differential element (packing) as shown in Figure 2 of the absorber is:

$$\left[ \begin{array}{l} \text{Rate of mass flow of} \\ \text{component } i \text{ into} \\ \text{differential element} \end{array} \right] = \left[ \begin{array}{l} \text{Rate of mass flow of} \\ \text{component } i \text{ out of} \\ \text{differential element} \end{array} \right] + \left[ \begin{array}{l} \text{Rate of mass of} \\ \text{component } i \text{ transfered} \\ \text{to component } i + 1 \text{ within} \\ \text{differential element} \end{array} \right] \quad (5)$$

The various terms in equation (5) were obtained as follows:

$$\begin{aligned} \text{Rate of mass flow of} \\ \text{component } i \text{ into} \\ \text{differential element} &= GAY_{CO_2} \\ \text{Rate of mass flow of} \\ \text{component } i \text{ out of} \\ \text{differential element} &= GAY_{CO_2} + GAdY_{CO_2} \\ \text{Rate of mass of} \\ \text{component } i \text{ transfered} \\ \text{to component } i + 1 \text{ within} \\ \text{differential element} &= K_G(Y_{CO_2} - Y_{CO_2,e})adzA \end{aligned}$$

Substituting these expressions into mass balance equation yields:

$$GAY_{CO_2} = GAY_{CO_2} + GAdY_{CO_2} + K_G(Y_{CO_2} - Y_{CO_2,e})adzA \quad (6)$$

Simplifying yields:

$$\frac{dY_{CO_2}}{dz} = -\frac{K_G(Y_{CO_2} - Y_{CO_2,e})a}{G} \quad (7)$$

The same procedure can be followed to obtain the model equation for the solvent as:

$$\frac{dX_{MDEA}}{dz} = -\frac{K_G(X_{MDEA} - X_{MDEA,e})a}{G} \quad (8)$$

**B. ENERGY BALANCE**

The steady state energy balance on a differential element (packing) as shown in Figure 2 of the absorber is:

$$\left[ \begin{array}{l} \text{Rate of heat flow} \\ \text{into} \\ \text{differential element} \end{array} \right] = \left[ \begin{array}{l} \text{Rate of heat flow} \\ \text{out of} \\ \text{differential element} \end{array} \right] \pm \left[ \begin{array}{l} \text{Rate of heat flow due to} \\ \text{mass transfer from/into} \\ \text{differential element} \end{array} \right] + \left[ \begin{array}{l} \text{Rate of heat transfered} \\ \text{from gas/liquid to liquid/gas phase} \\ \text{in differential element} \end{array} \right] \quad (9)$$

**I. GAS PHASE**

The various terms in equation (9) were obtained for the gas phase as follows:

$$\begin{aligned} \text{Rate of heat flow into} \\ \text{differential element} &= AGH_G \\ \text{Rate of heat flow out} \\ \text{of differential element} &= AGH_G + AGdH_G \\ \text{Rate of heat flow due} \\ \text{to mass transfer out} \\ \text{of differential element} &= [GdY_{CO_2}C_{PCO_2}(T_G - T_0) + GdY_{CO_2}H_{OS}]A \\ &\quad [GdX_{MDEA}C_{PMDEA}(T_G - T_0) + GdX_{MDEA}H_V]A \\ \text{Rate of heat transfered} \\ \text{from gas to liquid phase} \\ \text{in differential element} &= q_G adz = h_G a(T_G - T_L)Adz \end{aligned}$$

Substituting these expressions in equation (9) gives:

$$AGH_G = AGH_G + AGdH_G + [GdY_{CO_2}C_{PCO_2}(T_G - T_0) + GdY_{CO_2}H_{OS}]A + [GdX_{MDEA}C_{PMDEA}(T_G - T_0) + GdX_{MDEA}H_V]A + h_G a(T_G - T_L)Adz \quad (10)$$

Simplifying equation (10) gives:

$$\begin{aligned} -AGdH_G = \\ [GdY_{CO_2}C_{PCO_2}(T_G - T_0) + GdY_{CO_2}H_{OS}]A + [GdX_{MDEA}C_{PMDEA}(T_G - T_0) + GdX_{MDEA}H_V]A + \\ h_G a(T_G - T_L)Adz \end{aligned} \quad (11)$$

But:

$$H_G = C_{PB}(T_G - T_0) + Y_{CO_2}C_{PCO_2}(T_G - T_0) + Y_{CO_2}H_{OS} + X_{MDEA}C_{PMDEA}(T_G - T_0) + X_{MDEA}H_V \quad (12)$$

$$dH_G = C_{PB}dT_G + Y_{CO_2}C_{PCO_2}dT_G + (C_{PCO_2}(T_G - T_0) + H_{OS})dY_{CO_2} + X_{MDEA}C_{PMDEA}dT_G + (C_{PMDEA}(T_G - T_0) + H_V)dX_{MDEA} \quad (13)$$

Substituting equation (13) into equation (11) gives:

$$\begin{aligned} -AG [C_{PB}dT_G + Y_{CO_2}C_{PCO_2}dT_G + (C_{PCO_2}(T_G - T_0) + H_{OS})dY_{CO_2} + X_{MDEA}C_{PMDEA}dT_G \\ + (C_{PMDEA}(T_G - T_0) + H_V)dX_{MDEA}] \\ = [GdY_{CO_2}C_{PCO_2}(T_G - T_0) + GdY_{CO_2}H_{OS}]A \\ + [GdX_{MDEA}C_{PMDEA}(T_G - T_0) + GdX_{MDEA}H_V]A \\ + h_Ga(T_G - T_L)Adz \end{aligned} \quad (14)$$

Expanding and rearranging equation (14) yields:

$$-AG (C_{PB} + Y_{CO_2}C_{PCO_2} + X_{MDEA}C_{PMDEA})dT_G = h_Ga(T_G - T_L)Adz \quad (15)$$

Equation (15) can be rearranged to give:

$$\frac{dT_G}{dz} = \frac{-h_Ga(T_G - T_L)}{G(C_{PB} + Y_{CO_2}C_{PCO_2} + X_{MDEA}C_{PMDEA})} \quad (16)$$

## II. LIQUID PHASE

The various terms in equation (9) were obtained for the liquid phase as follows:

$$\begin{aligned} \text{Rate of heat flow into differential element} &= (L + dL)(H_L + dH_L)A \\ \text{Rate of heat flow out of differential element} &= ALH_L \\ \text{Rate of heat flow due to mass transfer into differential element} &= -[GdY_{CO_2}C_{PCO_2}(T_G - T_0) + GdY_{CO_2}H_{OS}]A - [GdX_{MDEA}C_{PMDEA}(T_G - T_0) + GdX_{MDEA}H_V]A \\ \text{Rate of heat transferred from liquid to gas phase in differential element} &= -q_Gadz = -h_Ga(T_G - T_L)Adz \end{aligned}$$

Substituting these expressions into equation (9) gives:

$$(L + dL)(H_L + dH_L)A - [GdY_{CO_2}C_{PCO_2}(T_G - T_0) + GdY_{CO_2}H_{OS}]A - [GdX_{MDEA}C_{PMDEA}(T_G - T_0) + GdX_{MDEA}H_V]A = ALH_L - h_Ga(T_G - T_L)Adz \quad (17)$$

Simplifying equation (17) yields:

$$LdH_L = [GC_{PCO_2}(T_G - T_0) + GH_{OS}]dY_{CO_2} + [GC_{PMDEA}(T_G - T_0) + GH_V]dX_{MDEA} - h_Ga(T_G - T_L)dz \quad (18)$$

$$\text{Let } H_L = C_{PL}T_L \text{ and } dH_L = C_{PL}dT_L \quad (19)$$

Substituting equation (19) into (18) and rearranging yields:

$$LC_{PL} \frac{dT_L}{dz} = [GC_{PCO_2}(T_G - T_0) + GH_{OS}] \frac{dY_{CO_2}}{dz} + [GC_{PMDEA}(T_G - T_0) - GH_V] \frac{dX_{MDEA}}{dz} - h_Ga(T_G - T_L) \quad (20)$$

Substituting equations (7) and (8) into equation (20) and rearranging gives:

$$\frac{dT_L}{dz} = -[GC_{PCO_2}(T_G - T_0) + GH_{OS}] \frac{K_G(Y_{CO_2} - Y_{CO_2,e})^a}{GLC_{PL}} - [GC_{PMDEA}(T_G - T_0) - GH_V] \frac{K_{MDEA}(X_{MDEA} - X_{MDEA,e})^a}{GLC_{PL}} - \frac{h_Ga(T_G - T_L)}{LC_{PL}} \quad (21)$$